Published in final edited form as:
Cancer Res. 2010 August 1; 70(15): 6313–6324. doi:10.1158/0008-5472.CAN-10-0999.

Vorinostat and sorafenib increase CD95 activation in gastrointestinal tumor cells through a Ca2+ - de novo ceramide - PP2A - ROS dependent signaling pathway

Margaret A. Park[1], **Clint Mitchell**[1], **Guo Zhang**[1], **Adly Yacoub**[1], **Jeremy Allegood**[1], **Dieter Häussinger**[6], **Roland Reinehr**[6], **Andrew Larner**[1], **Sarah Spiegel**[1], **Paul B. Fisher**[3,4], **Christina Voelkel-Johnson**[5], **Besim Ogretmen**[5], **Steven Grant**[1,2,3], and **Paul Dent**[1,3,*]

[1] Department of Biochemistry, Virginia Commonwealth University, 401 College St., Richmond, VA 23298

[2] Department of Medicine, Virginia Commonwealth University, 401 College St., Richmond, VA 23298

[3] VCU Institute of Molecular Medicine, Virginia Commonwealth University, 401 College St., Richmond, VA 23298

[4] Human and Molecular Genetics, Virginia Commonwealth University, 401 College St., Richmond, VA 23298

[5] Medical University of South Carolina, 173 Ashley Avenue, Charleston, SC 29425

[6] Clinic for Gastroenterology, Hepatology and Infectiology, Heinrich-Heine-University Düsseldorf, Düsseldorf, Germany

Abstract

The targeted therapeutics sorafenib and vorinostat interact in a synergistic fashion to kill carcinoma cells by activating CD95, and this drug combination is entering phase I evaluation. In this study we determined how CD95 is activated by treatment with this drug combination. Low doses of sorafenib and vorinostat but not the individual drugs rapidly increased ROS, Ca2+ and ceramide levels in GI tumor cells. The production of ROS was reduced in Rho zero cells. Quenching ROS blocked drug-induced CD95 surface localization and apoptosis. ROS generation, CD95 activation and cell killing was also blocked by quenching of induced Ca2+ levels or by inhibition of PP2A. Inhibition of acidic sphingomyelinase or de novo ceramide generation blocked the induction of ROS however combined inhibition of both acidic sphingomyelinase and de novo ceramide generation was required to block the induction of Ca2+. Quenching of ROS did not impact on drug-induced ceramide/dihydro-ceramide levels whereas quenching of Ca2+ reduced the ceramide increase. Sorafenib and vorinostat treatment radiosensitized liver and pancreatic cancer cells, an effect that was suppressed by quenching ROS or knock down of LASS6. Further, sorafenib and vorinostat treatment suppressed the growth of pancreatic tumors in vivo. Our findings demonstrate that induction of cytosolic Ca2+ by sorafenib and vorinostat is a primary event that elevates dihydroceramide levels, each essential steps in ROS generation that promotes CD95 activation.

[*]Correspondence to: Paul Dent, Ph.D., Department of Biochemistry and Molecular Biology, 401 College Street, Massey Cancer Center, Room 280a, Box 980035, Virginia Commonwealth University, Richmond VA 23298-0035. Tel: 804 628 0861, Fax: 804 827 1309, pdent@vcu.edu.

Introduction

In the United States, hepatoma and pancreatic carcinomas have 5 year survival rates of less than 10% and less than 5%, respectively (1,2). These statistics emphasize the need to develop novel therapies against these lethal malignancies.

The extracellular signal–regulated kinase 1/2 (ERK1/2) pathway is frequently dysregulated in neoplastic transformation (3–5). The ERK1/2 module comprises, along with c-Jun NH_2-terminal kinase (JNK1/2) and p38 MAPK, members of the MAPK super-family. These kinases are involved in responses to diverse mitogens and stresses and have also been implicated in survival processes. Activation of the ERK1/2 pathway is generally associated with survival whereas induction of JNK1/2 and p38 MAPK pathways generally signals apoptosis. Although the mechanisms by which ERK1/2 activation promote survival are not fully characterized, a number of anti-apoptotic effector proteins have been identified, including increased expression of anti-apoptotic proteins such as c-FLIP (6–11).

Sorafenib is a multi-kinase inhibitor that was originally developed as an inhibitor of Raf-1, but which was subsequently shown to inhibit multiple other kinases, including class III tyrosine kinase receptors such as platelet-derived growth factor, vascular endothelial growth factor receptors 1 and 2, c-Kit and FLT3 (12–14). Anti-tumor effects of sorafenib in renal cell carcinoma and in hepatoma have been ascribed to anti-angiogenic actions of this agent through inhibition of the growth factor receptors (15–17). Several groups have shown *in vitro* that sorafenib kills human leukemia cells at concentrations below the maximum achievable dose (C_{max}) of 15–20 μM, through a mechanisminvolving down-regulation of the anti-apoptotic BCL-2 family member MCL-1 (18,19). In these studies sorafenib-mediated MCL-1 down-regulation occurred through a translational rather than a transcriptional or post-translational process that was mediated by endoplasmic reticulum (ER) stress signaling (20,21). This suggests that the previously observed anti-tumor effects of sorafenib are mediated by a combination of inhibition of *Raf* family kinases; receptor tyrosine kinases that signal angiogenesis; and the induction of ER stress signaling.

Histone deacetylase inhibitors (HDACI) represent a class ofagents that act by blocking histone de-acetylation, thereby modifying chromatin structure and gene transcription. HDACIs promote histone acetylation and neutralization of positively charged lysine residues onhistone tails, allowing chromatin to assume a more open conformation, which favors transcription (22). HDACIs also induce acetylation of other non-histone targets, actions that may have plieotropic biological consequences, including inhibition of HSP90 function, induction of oxidative injury and up-regulation of death receptor expression (23–25). With respect to combinatorial drug studies with a multi-kinase inhibitor such as sorafenib, HDACIs are of interest in that they also down-regulate multiple oncogenic kinases by interfering with HSP90 function, leading to proteasomal degradation of these proteins. Vorinostat (Zolinza™) is a hydroxamic acid HDACI that has shown preliminary pre-clinical evidence of activity in hepatoma and other malignancies with a C_{max} of ~9 μM (26–28).

We have recently published that sorafenib and vorinostat to interact to kill in a wide range of tumor cell types via activation of the CD95 extrinsic apoptotic pathway (29,30). The present studies have extended in greater molecular detail our analyses to understanding how sorafenib and vorinostat interact to promote CD95 activation.

Materials and Methods

Materials

Sorafenib tosylate (Bayer) and vorinostat (Merck) were provided by the Cancer Treatment and Evaluation Program, NCI/NIH(Bethesda, MD). Commercially available validated short hairpin RNA molecules to knock down RNA/protein levels were from Qiagen (Valencia, CA): CD95 (SI02654463; SI03118255). The kit to assay PP2A activity was purchased from Millipore (Billerica, MA). Reagents and performance of experimental procedures were described in (20,21,29–37).

Cell line authentication

HEPG2, HEP3B, Mia PaCa2, PANC1 cells were purchased from the ATCC on a regular basis (fresh cryo-preserved vials of cells have been purchased at least once every 6 months). Cells have not been authenticated in the corresponding author's laboratory.

Methods

Culture and in vitro exposure of cells to drugs—Cells were cultured as described (29–32).

In vitro cell treatments—Cells were isolated at the indicated times, and subjected to trypan blue cell viability assay by counting in a light microscope or alternatively, Annexin V/propidium iodide assays were carried to confirm our cell viability data (29–32).

Transfection of cells with siRNA or with plasmids—Transfections were performed as described in (29–32).

Assessment of ROS Generation and cytosolic Ca^{2+} Levels—Cancer cells were plated in 96 well plates. Cells were pre-incubated with dihydro-DCF (5mM for 30minutes). Fluorescence measurements were obtained 0–30 minutes after drug addition with a Vector 3 plate reader. Data are presented corrected for basal uorescence of vehicle-treated cells at each time point and expressed as a –Fold increase in ROS levels. Carcinoma cells, seeded in 96 well plates, with fura-2 acetoxymethylester (fura-2) as an indicator. The ratio of Fura-2 emissions, when excited at the wavelengths of 340 and 380 nm, was recorded and analysis software were used to process and statistical analyze data.

Mass spectrometric analysis of sphingolipids and metabolites—Cells were washed extensively with PBS and detached by trypsinization. An aliquot of cells was taken for protein determination. For the remainder of cells, internal standards were added, lipids extracted, and individual ceramide acyl chain species were quantified by liquid chromatography, electrospray ionization tandem mass spectrometry (29).

Recombinant adenoviral vectors; infection in vitro—Cells were infected with adenoviruses at an approximate m.o.i. of 50 (29–32).

Animal studies—Mia Paca2 cells were injected S.C. (1×10^7) and 14 days later tumor volume determined by calipers. Animals were segregated into four groups of approximate mean tumor volume +/− SEM and then treated by oral gavage with vehicle or sorafenib +vorinostat. Animals are treated once per day for 5 consecutive days. Twenty four h after the first drug administration animals are placed in a shielded container and either mock exposed or have the flanks irradiated (2 Gy). Forty eight h after the first irradiation, a second irradiation (2 Gy) is performed. Tumors were subjected to two cycles of drug treatment/

radiation exposure (total dose 4 × 2 Gy). Tumor mass is determined at least every third day after the initiation of drug treatment.

Data analysis—Comparison of the effects of various treatments was performed using ANOVA and the Student's t test. Differences with a *p*-value of < 0.05 were considered statistically significant. All experiments were performed on at least two separate occasions and: each cell death or ceramide measurement experiment had between 3 and 4 separate independent experimental data points per experiment; each ROS or Ca^{2+} measurement had at least 8–12 independent data points per experiment. Thus experiments shown are the means of multiple individual data points per experiment from multiple experiments (± SEM).

Results

Treatment of cells with low concentrations of sorafenib and vorinostat, but not the individual agents, promoted activation of CD95 and the generation of reactive oxygen species (ROS) (Figures 1A and 1B). The rapid activation of CD95 was not reduced by incubation with a neutralizing antibody to inhibit FAS ligand (not shown). The production of ROS was quenched using N-acetyl cysteine or MnTBAP (Figure 1C). Mitochondria deficient rho zero HuH7 cells were generated (29–32); cells lacking functional mitochondria exhibited a significantly reduced ability to generate ROS in response to sorafenib and vorinostat exposure (Figure 1D).

Quenching of drug-induced ROS suppressed sorafenib and vorinostat toxicity (Figures 2A and 2B). Quenching of ROS also suppressed CD95 activation (Figure 2B, inset panel). Molecular quenching of ROS using thioredoxin (TRX) suppressed ROS generation, CD95 activation and drug toxicity whereas molecular enhancement of ROS generation via expression of a mutant inactive TRX protein enhanced ROS generation, though not CD95 activation, and promoted drug toxicity (Figure 2C). HuH7 hepatoma cells do not express CD95 and are relatively resistant to sorafenib and vorinostat –induced cell killing (29). Transfection of HuH7 cells with a wild type CD95-YFP construct, but not a construct lacking two known sites of regulatory tyrosine phosphorylation CD95-YFP FF, facilitated sorafenib and vorinostat toxicity (Figure 2D). Sorafenib and vorinostat treatment promoted tyrosine phosphorylation and cell surface localization of wild type CD95-YFP but not of CD95-YFP YY-FF (Figure 2D, not shown).

Low concentrations of either sorafenib (1–3 μM) or vorinostat (250–500 nM) did not strongly increase either: ROS or Ca^{2+} levels whereas we did observe, at 9–12 μM sorafenib and > 1 μM vorinostat concentrations measurable effects of the individual drugs on ROS and Ca^{2+} levels (data not shown). Treatment of tumor cells with low doses of sorafenib and vorinostat enhanced cytosolic Ca^{2+} levels (Figure 3A). Quenching of ROS did not block drug –induced cytosolic Ca^{2+} levels (Figure 3B). Quenching of Ca^{2+}, using either BAPTA-AM or expression of Calbindin D28, blocked drug-induced ROS induction (Figure 3C, not shown). Expression of Calbindin D28 blocked endogenous CD95 surface localization, CD95 tyrosine phosphorylation and CD95 association with caspase 8 (Figure 3D, upper section). Expression of Calbindin D28 blocked sorafenib and vorinostat toxicity (Figure 3D, lower graph). Knock down of CD95 neither blocked drug –induced cytosolic Ca^{2+} levels nor blocked capacitative Ca^{2+} entry into cells (Figures S1–S3).

Prior studies using sorafenib and vorinostat had implicated ceramide as a mediator of CD95 activation. Loss of acidic sphingomyelinase expression (ASMase −/−) caused a partial though statistically significant ($p < 0.05$) reduction in drug –induced cytosolic Ca^{2+} levels (Figure 4A). In contrast to the partial effect observed on reducing Ca^{2+} levels, deletion of

ASMase expression abolished drug –induced ROS production (Figure 4B). Knock down of ASMase or inhibition of the de novo ceramide synthase pathway each caused a partial reduction in drug –induced cytosolic Ca^{2+} levels, and complete blockade of ceramide generation abolished Ca^{2+} induction (Figure 4C). Combined knock down of ASMase expression and inhibition of de novo ceramide synthesis in hepatoma cells abolished sorafenib and vorinostat –induced ROS levels (Figure 4D).

We next wished to place the sequence of ceramide generation within the context of elevated ROS and Ca^{2+} levels. Knock down of CD95 protected tumor cells from sorafenib +vorinostat toxicity (Figure 5A). CD95 activation and sorafenib+vorinostat toxicity were blocked by knock down of ASMase and by inhibition of de novo ceramide synthesis (Figure 5B). Knock down of ceramide synthase 6 (LASS6) expression abolished drug-induced activation of CD95 and significantly reduced drug toxicity (Figure 5C). Inhibition of ROS generation did not alter sorafenib+vorinostat –induced C16 ceramide or dihydro-ceramide levels (Figure 5D). However, inhibition of drug –induced cytosolic Ca^{2+} levels or knock down of LASS6 significantly reduced the amount of C16 dihydro-ceramide generated following drug treatment (Figure 5D, not shown). In parallel studies using SW620 colon cancer cells that lack LASS6 expression, transfected to express LASS6, we noted that re-expression of ceramide synthase 6 restored drug-induced ROS generation levels (Figure S4).

As sorafenib+vorinostat exposure generated ceramide, and the protein serine/threonine phosphatase PP2A in can play a pivotal role in ceramide-dependent signaling, as well as in the regulation of ROS generation, we determined whether modulation of PP2A function impacted on the actions of this drug combination (29,37). Sorafenib and vorinostat activated PP2A in a LASS6-dependent fashion (Figure 6A). Expression of a wild type PP2A inhibitory protein (IPP2A) whose function can be blocked by ceramide or a mutant inhibitor protein whose function cannot be altered by ceramide suppressed drug combination –induced ROS generation and cell death (Figures 6B and 6C). Phosphorylation of mitochondria localized STAT3 S727 plays a key role in regulating the rate of mitochondrial respiration, and *de facto*, mitochondrial ROS production, and STAT3 S727 is a PP2A substrate (38). Sorafenib and vorinostat treatment reduced STAT3 S727 phosphorylation by ~50% within 2h (Figure 6D). Expression of a dominant negative form of STAT3 S727A enhanced sorafenib and vorinostat lethality whereas expression of activated STAT3 S727D suppressed drug toxicity (Figure 6D).

Sorafenib and HDACI drug combination therapy is entering clinical phase I evaluation. Radiotherapy is known to generate ROS and ceramide, and it is a primary therapeutic modality for pancreatic cancer. Sorafenib and vorinostat treatment radiosensitized pancreatic and liver cancer cells in vitro (Figures S5 and S6). Radiosensitization was blocked by expression of TRX or knock down of LASS6 expression (Figure S5). Treatment of animals carrying MiaPaca2 tumors with sorafenib and vorinostat significantly reduced tumor growth in vivo, which validates this drug combination as a possible therapeutic for pancreatic cancer (Figure S7; $p < 0.05$). Tumor growth was blunted by radiation exposure however radiation exposure did not significantly further enhance the anti-tumor effects of sorafenib and vorinostat treatment on tumor re-growth. Further studies will be required to determine whether the in vivo administration of radiotherapy combined with drug treatment is schedule dependent.

Discussion

The present studies attempted to determine in detail the molecular mechanisms by which sorafenib and vorinostat interacted to activate CD95 and promote drug-induced toxicity.

Low concentrations of sorafenib and vorinostat interacted in a greater than additive manner to increase ROS levels. The induction of ROS occurred in cells lacking expression of CD95 strongly arguing against death receptor –induced activation of NADPH oxidases in this process. In rho zero cells the induction of ROS was reduced, arguing that mitochondria represent the major source of drug-induced ROS generation. Quenching of ROS blocked CD95 activation and drug combination –induced cell death. Sorafenib and vorinostat treatment increased cytosolic Ca^{2+} levels in an ROS –independent fashion and quenching of Ca^{2+} blocked the increase in ROS levels, CD95 activation and tumor cell killing. Inhibition of ASMase or of de novo ceramide generation almost abolished drug combination –induced ROS levels and CD95 activation but individually blockade of either pathway only caused a partial suppression in drug –induced cytosolic Ca^{2+}. Quenching of Ca^{2+}, or knock down of ceramide synthase 6, reduced drug –induced ceramide levels. Thus our data argues for drug combination –induced Ca^{2+} signaling (primary) and ceramide generation (secondary) as two interdependent signaling processes that regulate each other, and that both signals act in concert to promote ROS generation which is essential for drug-induced CD95 activation and tumor cell death (Figure S8).

Bile acids can promote ligand independent, ASMase and ceramide –dependent, activation of CD95 in hepatocytes (11,34–39). The generation of ceramide has been shown by many groups to promote ligand independent activation of growth factor receptors via the clustering of these receptors and other signal facilitating proteins into lipid rich domains (39). The six known ceramide synthase genes (LASS) are localized in the ER and different LASS proteins have been noted to generate different chain length ceramide forms (40). Based on our data, with increases in C16 dihydro-ceramide levels, it was probable that vorinostat and sorafenib were modulating the activities of LASS6 and LASS5, respectively (40). We identified ceramide synthase 6 (LASS6) as an essential enzyme in the drug-induced induction of ceramide, CD95 activity and in tumor cell killing. Treatment of cells with vorinostat increased the acetylation of LASS6, suggesting that one mechanism of drug-induced LASS6 activity may be mediated in part via this process (Unpublished observations). It is well known that other non-histone proteins are functionally regulated by reversible acetylation, notably NFκB and HSP90 (22–25). Additional studies will be required to define the precise site of acetylation in LASS6 and to discover whether it truly is a site of regulatory acetylation.

The generation of ROS was significantly reduced in rho zero cells, and we have documented a key role for mitochondria in the production of ROS in response to various agents (e.g. 41). In the present studies ROS production was a tertiary effect dependent on the actions of ceramide and Ca^{2+}. It has been widely documented that the release of Ca^{2+} from the ER in to the cytosol rapidly alters Ca^{2+} levels in mitochondria; and that changes in Ca^{2+} fluxes within mitochondria can stimulate ROS production (e.g. 42). Ceramide levels, independently of Ca^{2+} fluxes, are causal in regulating mitochondrial ROS production, and we noted that whereas inhibition of both ASMase and de novo ceramide generation was required to suppress Ca^{2+} signaling, inhibition of either de novo or ASMase actions blocked ROS production. There are several probable modes of ceramide action at the mitochondrion that could alter respiratory chain complex activities, including modulation of membrane fluidity as well as activation of PP2A (37,43–45). The mitochondrial respiratory chain complexes, as well as BCL-2 family proteins, are heavily Ser/Thr phosphorylated and ceramide has the potential to regulate their function via PP2A. In this regard, drug treatment reduced STAT3 S727 phosphorylation and inhibition of PP2A activity blocked sorafenib + vorinostat –induced ROS, and suppressed drug toxicity. The additional molecular targets of PP2A beyond STAT3 in the regulation of mitochondrial ROS generation will be explored in future studies.

Ligand independent activation of CD95 is a complex process, including tyrosine phosphorylation, altered sub-cellular localization and formation of the DISC i.e. association with FADD and pro-caspase 8 (37,38). In our system drug-induced activation of CD95, as defined by formation of the DISC or by plasma membrane localization of CD95, was blocked by quenching of Ca^{2+}, suppressing ceramide formation or by quenching ROS production. Tyrosine phosphorylation of CD95 was essential for drug-induced membrane localization and DISC formation, but tyrosine phosphorylation of CD95 was only suppressed by quenching Ca^{2+}. Thus at least two independent signals downstream of drug-induced Ca^{2+} signaling act to promote ligand independent activation of CD95 in GI tumor cells. The regulation of CD95 tyrosine phosphorylation has been proposed to be catalyzed by ERBB1 and by Src family tyrosine kinases (38).

An additional question which remains unresolved is how sorafenib and vorinostat treatment promote Ca^{2+} signaling, and what the putative primary effectors for these drugs are. Two likely targets of sorafenib and vorinostat may be LASS6 and the IP_3 receptors that regulate ER Ca^{2+} fluxes. At present little is known about how the ceramide synthase proteins are enzymatically regulated and it is possible that sorafenib reduces phosphorylation at a regulatory site or alternatively that vorinostat promotes LASS6 acetylation which facilitates enzyme activation. Whether Ca^{2+} - calmodulin signaling directly or via CaM kinase actions modulates ceramide synthase function is unknown. It is also possible that the drug combination causes inactivation of ceramidase enzyme activities that act to lower ceramide levels. IP_3 levels are regulated by phospholipase C and phosphodiesterase enzymes; at present the impact of sorafenib and vorinostat exposure on the activities of PLC enzymes is unclear and data from many groups arguing that sorafenib inhibits receptor tyrosine kinases such as the PDGF and VEGF receptors and c-Kit would *a priori* predict for reduced activity of PLC enzymes that would reduce IP_3 levels (14,15).

Sorafenib and HDACI combination therapy is entering phase I evaluation at both VCU and at MUSC in a variety of solid and liquid tumor types. We have noted that sorafenib and vorinostat combination therapy demonstrates in vitro efficacy against multiple pancreatic cancer cell lines (29,30,46). The present studies demonstrated that sorafenib and vorinostat treatment suppressed the growth of pancreatic tumor cells in vivo, potentially validating this drug combination as a new therapeutic for pancreatic cancer. Further studies, however, will be required to determine whether sorafenib and HDACI combination therapy can radiosensitize GI tumors in a sequence dependent fashion in vivo.

Supplementary Material

Refer to Web version on PubMed Central for supplementary material.

Acknowledgments

This work was funded; to P.D. from PHS grants (R01-DK52825, P01-CA104177, R01-CA108520).

References

1. Parkin DM, Bray F, Ferlay J, Pisani P. Global cancer statistics, 2002. CA Cancer J Clin 2005;55:74–108. [PubMed: 15761078]
2. Bilimoria KY, Bentrem DJ, Lillemoe KD, Talamonti MS, Ko CY. Pancreatic Cancer Quality Indicator Development Expert Panel, American College of Surgeons. Assessment of pancreatic cancer care in the United States based on formally developed quality indicators. J Natl Cancer Inst 2009;101:848–59. [PubMed: 19509366]

3. Dent, P. MAP kinase pathways in the control of hepatocyte growth, metabolism and survival. In: Dufour, JF.; Clavien, P-A., editors. Signaling Pathways in Liver Diseases. Vol. Chapter 19. Springer Press; 2005. p. 223-238.
4. Dent P, Yacoub A, Fisher PB, Hagan MP, Grant S. MAPK pathways in radiation responses. Oncogene 2003;22:5885–96. [PubMed: 12947395]
5. Valerie K, Yacoub A, Hagan MP, et al. Radiation-induced cell signaling: inside-out and outside-in. Mol Cancer Ther 2007;6:789–801. [PubMed: 17363476]
6. Grant S, Dent P. Kinase inhibitors and cytotoxic drug resistance. Clin Cancer Res 2004;10:2205–7. [PubMed: 15073093]
7. Allan LA, Morrice N, Brady S, Magee G, Pathak S, Clarke PR. Inhibition of caspase-9 through phosphorylation at Thr 125 by ERK MAPK. Nat Cell Biol 2003;5:647–54. [PubMed: 12792650]
8. Mori M, Uchida M, Watanabe T, et al. Activation of extracellular signal-regulated kinases ERK1 and ERK2 induces Bcl-xL up-regulation via inhibition of caspase activities in erythropoietin signaling. J Cell Physiol 2003;195:290–7. [PubMed: 12652655]
9. Ley R, Balmanno K, Hadfield K, Weston C, Cook SJ. Activation of the ERK1/2 signaling pathway promotes phosphorylation and proteasome-dependent degradation of the BH3-only protein, Bim. J Biol Chem 2003;278:18811–6. [PubMed: 12646560]
10. Wang YF, Jiang CC, Kiejda KA, Gillespie S, Zhang XD, Hersey P. Apoptosis induction in human melanoma cells by inhibition of MEK is caspase-independent and mediated by the Bcl-2 family members PUMA, Bim, and Mcl-1. Clin Cancer Res 2007;13:4934–42. [PubMed: 17652623]
11. Qiao L, Han SI, Fang Y, et al. Bile acid regulation of C/EBPbeta, CREB, and c-Jun function, via the extracellular signal-regulated kinase and c-Jun NH2-terminal kinase pathways, modulates the apoptotic response of hepatocytes. Mol Cell Biol 2003;23:3052–66. [PubMed: 12697808]
12. Li N, Batt D, Warmuth M. B-Raf kinase inhibitors for cancer treatment. Curr Opin Investig Drugs 2007;8:452–6.
13. Davies BR, Logie A, McKay JS, et al. AZD6244 (ARRY-142886), a potent inhibitor of mitogen-activated protein kinase/extracellular signal-regulated kinase kinase 1/2 kinases: mechanism of action in vivo, pharmacokinetic/pharmacodynamic relationship, and potential for combination in preclinical models. Mol Cancer Ther 2007;6:2209–19. [PubMed: 17699718]
14. Flaherty KT. Sorafenib: delivering a targeted drug to the right targets. Expert Rev Anticancer Ther 2007;7:617–26. [PubMed: 17492926]
15. Rini BI. Sorafenib. Expert Opin Pharmacother 2006;7:453–61. [PubMed: 16503817]
16. Strumberg D. Preclinical and clinical development of the oral multikinase inhibitor sorafenib in cancer treatment. Drugs Today (Barc) 2005;41:773–84. [PubMed: 16474853]
17. Gollob JA. Sorafenib: scientific rationales for single-agent and combination therapy in clear-cell renal cell carcinoma. Clin Genitourin Cancer 2005;4:167–74. [PubMed: 16425993]
18. Rahmani M, Davis EM, Bauer C, Dent P, Grant S. Apoptosis induced by the kinase inhibitor BAY 43–9006 in human leukemia cells involves down-regulation of Mcl-1 through inhibition of translation. J Biol Chem 2005;280:35217–27. [PubMed: 16109713]
19. Rahmani M, Nguyen TK, Dent P, Grant S. The multikinase inhibitor sorafenib induces apoptosis in highly imatinib mesylate-resistant bcr/abl+ human leukemia cells in association with signal transducer and activator of transcription 5 inhibition and myeloid cell leukemia-1 down-regulation. Mol Pharmacol 2007;72:788–95. [PubMed: 17595328]
20. Dasmahapatra G, Yerram N, Dai Y, Dent P, Grant S. Synergistic interactions between vorinostat and sorafenib in chronic myelogenous leukemia cells involve Mcl-1 and p21CIP1 down-regulation. Clin Cancer Res 2007;13:4280–90. [PubMed: 17634558]
21. Rahmani M, Davis EM, Crabtree TR, et al. The kinase inhibitor sorafenib induces cell death through a process involving induction of endoplasmic reticulum stress. Mol Cell Biol 2007;27:5499–513. [PubMed: 17548474]
22. Gregory PD, Wagner K, Horz W. Histone acetylation and chromatin remodeling. Exp Cell Res 2001;265:195–202. [PubMed: 11302684]
23. Marks PA, Miller T, Richon VM. Histone deacetylases. Curr Opin Pharmacol 2003;3:344–351. [PubMed: 12901942]

24. Bali P, Pranpat M, Swaby R, et al. Activity of suberoylanilide hydroxamic Acid against human breast cancer cells with amplification of her-2. Clin Cancer Res 2005;11:6382–9. [PubMed: 16144943]
25. Kwon SH, Ahn SH, Kim YK, et al. Apicidin, a histone deacetylase inhibitor, induces apoptosis and Fas/Fas ligand expression in human acute promyelocytic leukemia cells. J Biol Chem 2002;277:2073–80. [PubMed: 11698395]
26. Pang RW, Poon RT. From molecular biology to targeted therapies for hepatocellular carcinoma: the future is now. Oncology 2007;72 (Suppl 1):30–44. [PubMed: 18087180]
27. Venturelli S, Armeanu S, Pathil A, et al. Epigenetic combination therapy as a tumor-selective treatment approach for hepatocellular carcinoma. Cancer 2007;109:2132–41. [PubMed: 17407132]
28. Wise LD, Turner KJ, Kerr JS. Assessment of developmental toxicity of vorinostat, a histone deacetylase inhibitor, in Sprague-Dawley rats and Dutch Belted rabbits. Birth Defects Res B Dev Reprod Toxicol 2007;80:57–68. [PubMed: 17294457]
29. Zhang G, Park MA, Mitchell C, Hamed H, Rahmani M, Martin AP, Curiel DT, Yacoub A, Graf M, Lee R, Roberts JD, Fisher PB, Grant S, Dent P. Vorinostat and sorafenib synergistically kill tumor cells via FLIP suppression and CD95 activation. Clin Cancer Res 2008;14:5385–99. [PubMed: 18765530]
30. Park MA, Zhang G, Martin AP, Hamed H, Mitchell C, Hylemon PB, Graf M, Rahmani M, Ryan K, Liu X, Spiegel S, Norris J, Fisher PB, Grant S, Dent P. Vorinostat and sorafenib increase ER stress, autophagy and apoptosis via ceramide-dependent CD95 and PERK activation. Cancer Biol Ther 2008;7:1648–62. [PubMed: 18787411]
31. Park MA, Zhang G, Mitchell C, Rahmani M, Hamed H, Hagan MP, Yacoub A, Curiel DT, Fisher PB, Grant S, Dent P. Mitogen-activated protein kinase kinase 1/2 inhibitors and 17-allylamino-17-demethoxygeldanamycin synergize to kill human gastrointestinal tumor cells in vitro via suppression of c-FLIP-s levels and activation of CD95. Mol Cancer Ther 2008;7:2633–48. [PubMed: 18790746]
32. Yacoub A, Park MA, Gupta P, et al. Caspase-, cathepsin- and PERK-dependent regulation of MDA-7/IL-24-induced cell killing in primary human glioma cells. Mol Cancer Ther 2008;7:297–313. [PubMed: 18281515]
33. Mitchell C, Park MA, Zhang G, Han SI, Harada H, Franklin RA, Yacoub A, Li PL, Hylemon PB, Grant S, Dent P. 17-Allylamino-17-demethoxygeldanamycin enhances the lethality of deoxycholic acid in primary rodent hepatocytes and established cell lines. Mol Cancer Ther 2007;6:618–32. [PubMed: 17308059]
34. Gupta S, Natarajan R, Payne SG, Studer EJ, Spiegel S, Dent P, Hylemon PB. Deoxycholic acid activates the c-Jun N-terminal kinase pathway via FAS receptor activation in primary hepatocytes. Role of acidic sphingomyelinase-mediated ceramide generation in FAS receptor activation. J Biol Chem 2001;279:5821–8. [PubMed: 14660582]
35. Qiao L, Studer E, Leach K, et al. Deoxycholic acid (DCA) causes ligand-independent activation of epidermal growth factor receptor (EGFR) and FAS receptor in primary hepatocytes: inhibition of EGFR/mitogen-activated protein kinase-signaling module enhances DCA-induced apoptosis. Mol Biol Cell 2001;12:2629–45. [PubMed: 11553704]
36. Zhang G, Park MA, Mitchell C, Walker T, Hamed H, Studer E, Graf M, Gupta S, Hylemon PB, Fisher PB, Grant S, Dent P. Multiple cyclin kinase inhibitors promote bile acid –induced apoptosis and autophagy in primary hepatocytes via p53 – CD95 –dependent signaling. J Biol Chem 2008;283:24343–58. [PubMed: 18614532]
37. Mukhopadhyay A, Saddoughi SA, Song P, Sultan I, Ponnusamy S, Senkal CE, Snook CF, Arnold HK, Sears RC, Hannun YA, Ogretmen B. Direct interaction between the inhibitor 2 and ceramide via sphingolipid-protein binding is involved in the regulation of protein phosphatase 2A activity and signaling. FASEB J 2009;23:751–63. [PubMed: 19028839]
38. Wegrzyn J, Potla R, Chwae YJ, Sepuri NB, Zhang Q, Koeck T, Derecka M, Szczepanek K, Szelag M, Gornicka A, Moh A, Moghaddas S, Chen Q, Bobbili S, Cichy J, Dulak J, Baker DP, Wolfman A, Stuehr D, Hassan MO, Fu XY, Avadhani N, Drake JI, Fawcett P, Lesnefsky EJ, Larner AC. Function of mitochondrial Stat3 in cellular respiration. Science 2009;323:793–7. [PubMed: 19131594]

39. Reinehr R, Häussinger D. Hyperosmotic activation of the CD95 system. Methods Enzymol 2007;428:145–60. [PubMed: 17875416]
40. Pewzner-Jung Y, Ben-Dor S, Futerman AH. When do Lasses (longevity assurance genes) become CerS (ceramide synthases)?: Insights into the regulation of ceramide synthesis. J Biol Chem 2006;281:25001–5. [PubMed: 16793762]
41. Rosato RR, Almenara JA, Maggio SC, Coe S, Atadja P, Dent P, Grant S. Role of histone deacetylase inhibitor-induced reactive oxygen species and DNA damage in LAQ-824/fludarabine antileukemic interactions. Mol Cancer Ther 2008;7:3285–97. [PubMed: 18852132]
42. Mikkelsen RB, Wardman P. Biological chemistry of reactive oxygen and nitrogen and radiation-induced signal transduction mechanisms. Oncogene 2003;22:5734–54. [PubMed: 12947383]
43. Roy SS, Madesh M, Davies E, Antonsson B, Danial N, Hajnóczky G. Bad targets the permeability transition pore independent of Bax or Bak to switch between Ca2+-dependent cell survival and death. Mol Cell 2009;33:377–88. [PubMed: 19217411]
44. White-Gilbertson S, Mullen T, Senkal C, Lu P, Ogretmen B, Obeid L, Voelkel-Johnson C. Ceramide synthase 6 modulates TRAIL sensitivity and nuclear translocation of active caspase-3 in colon cancer cells. Oncogene 2009;28:1132–41. [PubMed: 19137010]
45. Walker T, Mitchell C, Park MA, Yacoub A, Graf M, Rahmani M, Houghton PJ, Voelkel-Johnson C, Grant S, Dent P. Sorafenib and vorinostat kill colon cancer cells by CD95-dependent and -independent mechanisms. Mol Pharmacol 2009;76:342–55. [PubMed: 19483104]
46. Martin AP, Park MA, Mitchell C, Walker T, Rahmani M, Thorburn A, Häussinger D, Reinehr R, Grant S, Dent P. BCL-2 family inhibitors enhance histone deacetylase inhibitor and sorafenib lethality via autophagy and overcome blockade of the extrinsic pathway to facilitate killing. Mol Pharmacol 2009;76:327–41. [PubMed: 19483105]

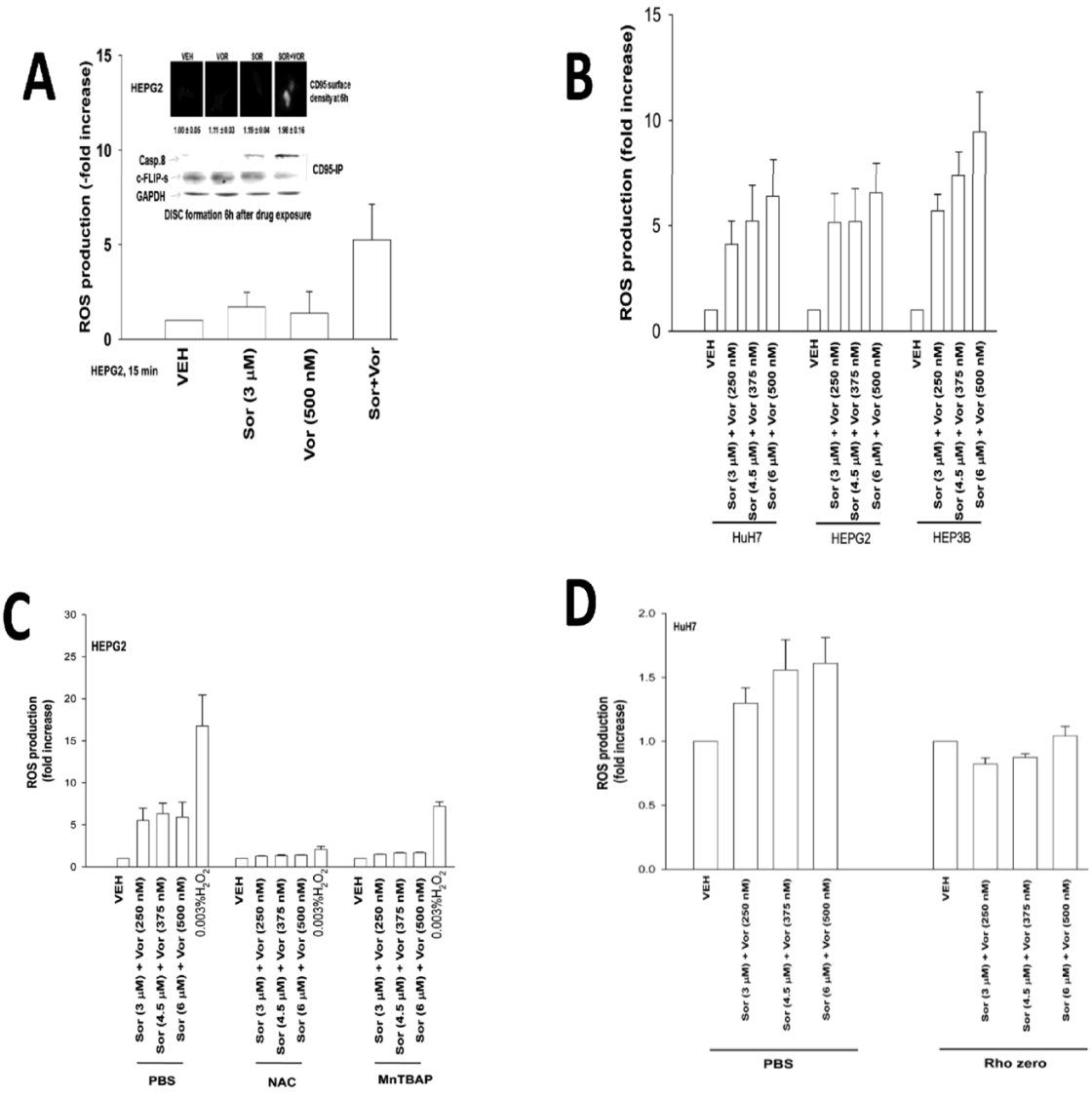

Figure 1. Sorafenib and vorinostat interact to increase ROS levels in GI tumor cells

Panel A. HEPG2 cells were treated with vehicle (DMSO), sorafenib (Sor), vorinostat (Vor) or in combination. ROS levels were measured 15 min after exposure and plotted as the –Fold increase (n = 2, +/− SEM). Upper: HEPG2 cells were treated with sorafenib, vorinostat or the combination and 6h after exposure cells were fixed and CD95 surface levels determined by IHC; HEPG2 cells were treated with vehicle (DMSO), sorafenib, vorinostat or the combination and 6h after exposure cells were lysed and CD95 immunoprecipitated followed by immunoblotting of the precipitate for DISC formation. **Panel B.** Cells were treated with vehicle (DMSO), sorafenib and vorinostat. ROS levels were measured 15 min after exposure and plotted as the –Fold increase (n = 2, +/− SEM). **Panel C.** HEPG2 cells were treated with vehicle (PBS), N-acetyl cysteine or MnTBAP followed 30 min later by sorafenib and vorinostat. ROS levels were measured 15 min after exposure and plotted as the –Fold increase (n = 2, +/− SEM). **Panel D.** HuH7 parental and rho zero hepatoma cells were treated with vehicle (DMSO), sorafenib and vorinostat. ROS levels were measured 15 min after exposure and plotted as the –Fold increase (n = 2, +/− SEM).

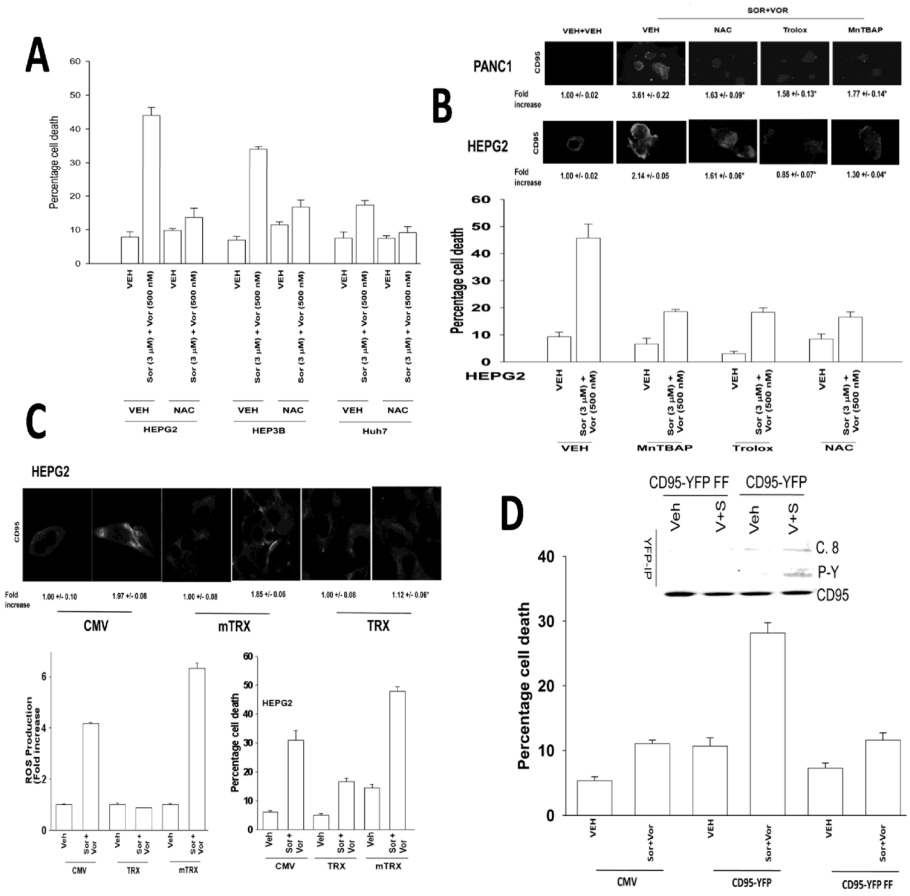

Figure 2. ROS play a central role in CD95 activation and apoptosis

Panel A. Hepatoma cells were pre-treated with N-acetyl cysteine and then with sorafenib and vorinostat. Viability was determined by trypan blue after 48h (n = 3, +/− SEM). **Panel B.** *Lower Panel:* HEPG2 cells were pre-treated with N-acetyl cysteine, Trolox or MnTBAP and with sorafenib and vorinostat. ROS levels were measured 15 min after exposure (n = 2, +/− SEM). *Upper IHC:* PANC1 and HEPG2 cells were pre-treated with N-acetyl cysteine, Trolox or MnTBAP and 30 min later treated with sorafenib and vorinostat. Cells were fixed after 6h and cell surface CD95 levels determined. **Panel C.** *Lower graphs:* Left: HEPG2 cells were transfected with empty vector (CMV) or to express either wild type Thioredoxin (TRX) or mutant inactive Thioredoxin (mTRX). Twenty-four h after transfection cells were treated with sorafenib (3.0 μM) and vorinostat (500 nM). ROS levels were measured 15 min after treatment (n = 2, +/− SEM); Right: HEPG2 cells were transfected to express either TRX or mTRX. Twenty-four h after transfection cells were treated with, sorafenib, vorinostat or both drugs. Cells were isolated after 48h and viability determined by trypan blue (n = 3, +/− SEM). *Upper IHC:* HEPG2 cells were transfected to express TRX or mTRX. Twenty-four h after transfection cells were treated with sorafenib and vorinostat. Six h after treatment cells were fixed and CD95 plasma membrane levels determined (n = 2, +/− SEM). **Panel D.** *Lower Graph*: HuH7 cells were transfected to express CD95-YFP or CD95-YFP FF. Twenty-four h after transfection cells were treated with sorafenib (3.0 μM) and vorinostat (500 nM). Cells were isolated after 48h and viability determined by trypan blue (n = 2, +/− SEM). *Upper section*: HuH7 cells were transfected to express CD95-YFP or CD95-YFP FF. Twenty-four h after transfection cells were treated with sorafenib and vorinostat.

Cells were isolated after 6h and CD95 immunoprecipitated to determine DISC formation and CD95 tyrosine phosphorylation.

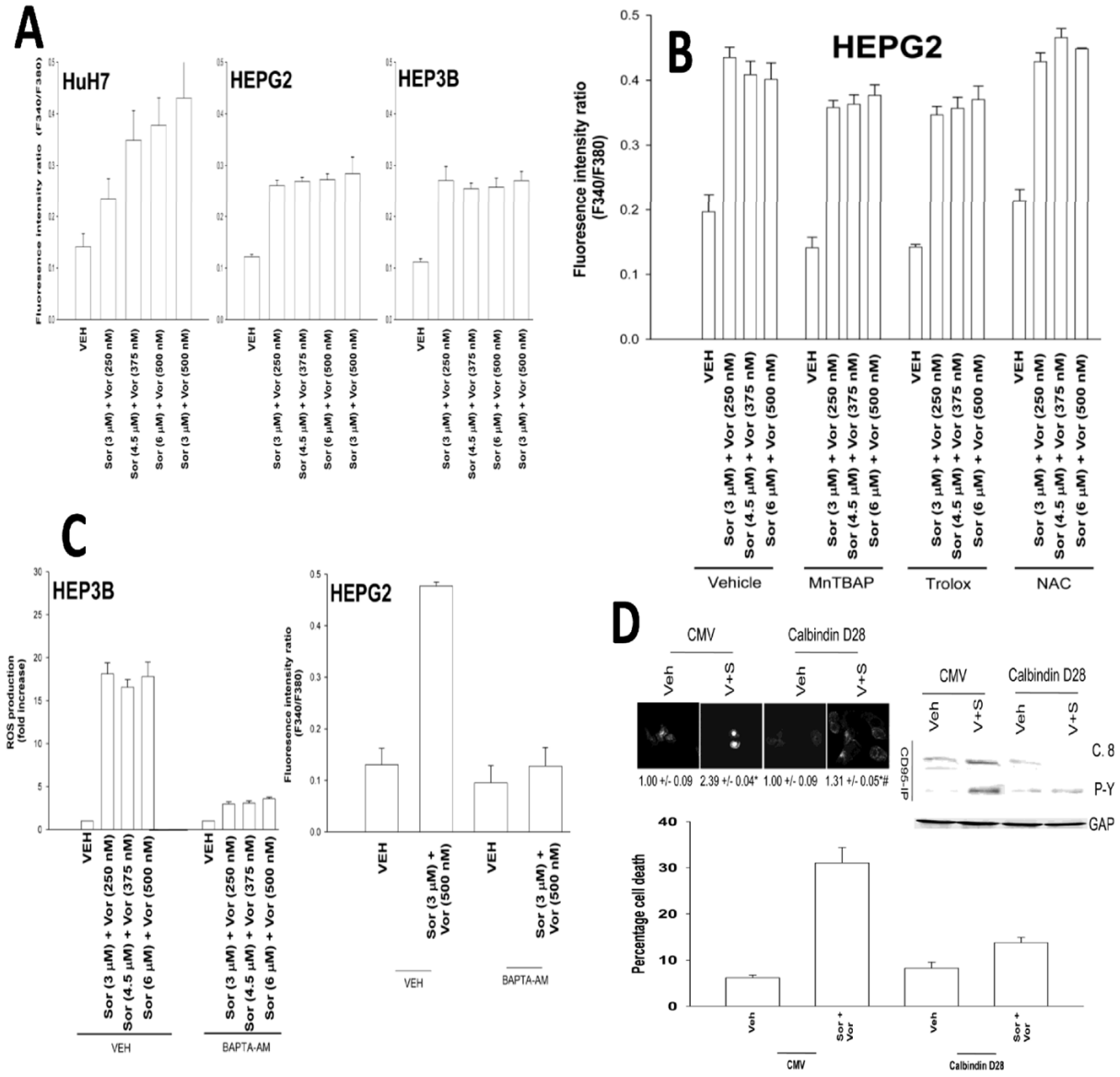

Figure 3. Sorafenib and vorinostat treatment modulates Ca^{2+} signaling

Panel A. Hepatoma cells were treated with sorafenib and vorinostat. Cytosolic Ca^{2+} levels were measured 15 min after exposure and plotted as the fluorescence intensity ratio (n = 2, +/− SEM). **Panel B.** HEPG2 cells were pre-treated with MnTBAP, N-acetyl cysteine or Trolox followed 30 min later by treatment with sorafenib and vorinostat. Cytosolic Ca^{2+} levels were measured 15 min after exposure (n = 2, +/− SEM). **Panel C.** *left section:* HEP3B cells were pre-incubated in Ca^{2+} free media for 1h prior to addition of BAPTA-AM or vehicle. Ten minutes after BAPTA-AM addition were treated with sorafenib and vorinostat or with $CaCl_2$. ROS levels were measured 15 min after exposure (n = 2, +/− SEM). *Right section:* HEPG2 cells were pre-incubated in Ca^{2+} free media for 1h prior to addition of BAPTA-AM or vehicle. Ten minutes after BAPTA-AM addition were treated with sorafenib and vorinostat. Cytosolic Ca^{2+} levels were measured 15 min after exposure (n = 2, +/− SEM). **Panel D.** *Upper CD95 IHC:* HEPG2 cells were transfected to express Calbindin D28 and 24h later were treated with sorafenib (3 μM) and vorinostat (500 nM). Six h after exposure cells were fixed and the levels of plasma membrane CD95 determined

(n = 2, +/− SEM). *Blotting:* HEPG2 cells were transfected to express Calbindin D28 and 24h later were treated with sorafenib and vorinostat. Six h after exposure cells were isolated and CD95 immunoprecipitated and DISC formation determined (n = 3). *Lower graph:* HEPG2 cells were transfected to express Calbindin D28 and 24h later were treated with sorafenib and vorinostat. Cells were isolated 48h later and viability determined by trypan blue (n = 2, +/− SEM).

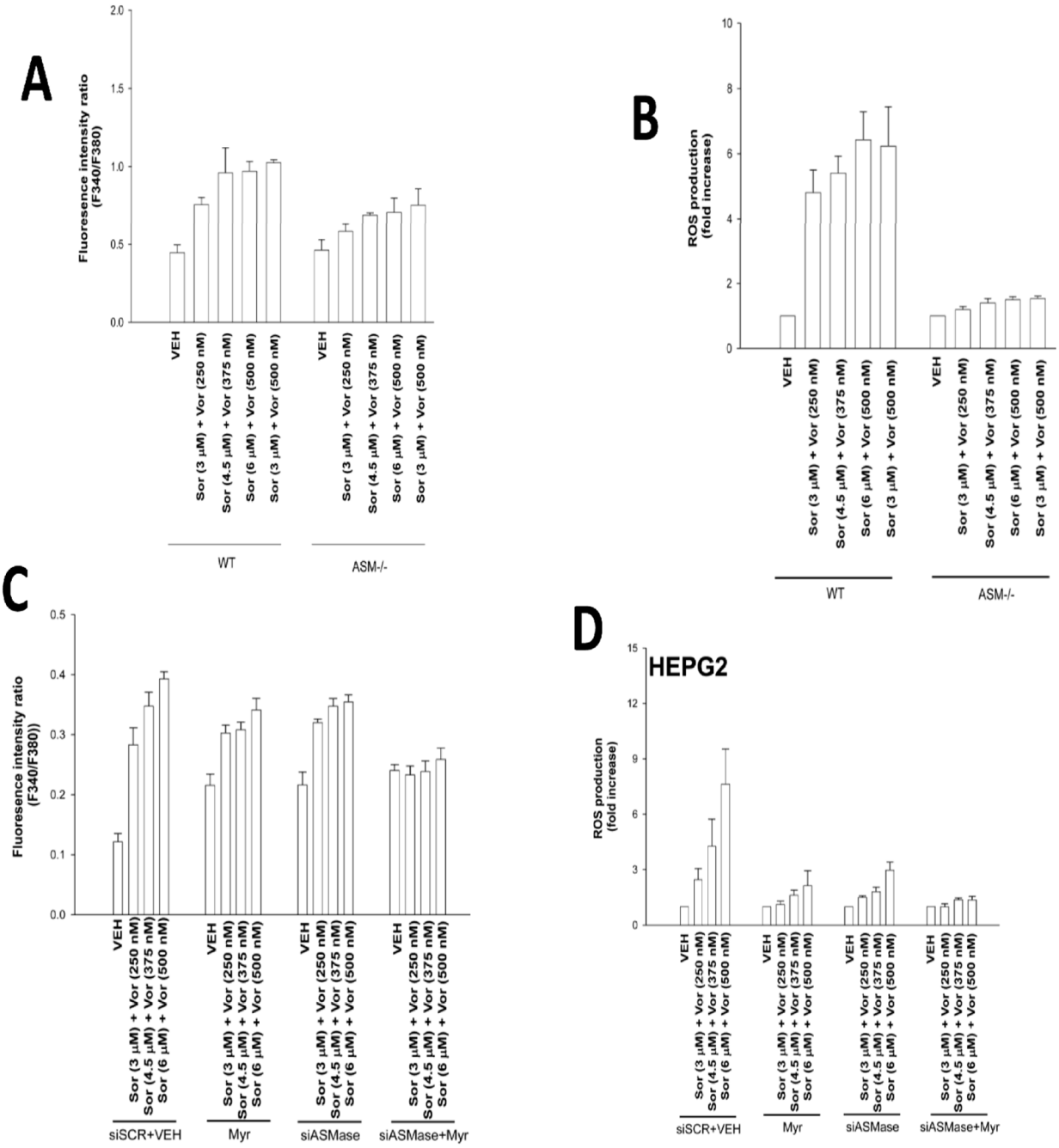

Figure 4. ROS generation is ceramide dependent

Panel A. Primary mouse hepatocytes (wild type and acidic sphingomyelinase null) were treated with sorafenib and vorinostat. Cytosolic Ca^{2+} levels were measured 15 min after exposure (n = 2, +/− SEM). **Panel B.** Primary mouse hepatocytes were treated with sorafenib and vorinostat. ROS levels were measured 15 min after drug exposure (n = 2, +/− SEM). **Panel C.** HEPG2 cells were transfected with an siRNA to knock down ASMase. Twenty-four h later cells were treated with myriocin, and were then treated with sorafenib and vorinostat. Cytosolic Ca^{2+} levels were measured 15 min after drug exposure (n = 2, +/− SEM). **Panel D.** HEPG2 cells were transfected with an siRNA to knock down ASMase. Twenty-four h later cells were treated with myriocin as indicated, and were then treated with

sorafenib and vorinostat. ROS levels were measured 15 min after drug exposure (n = 2, +/− SEM).

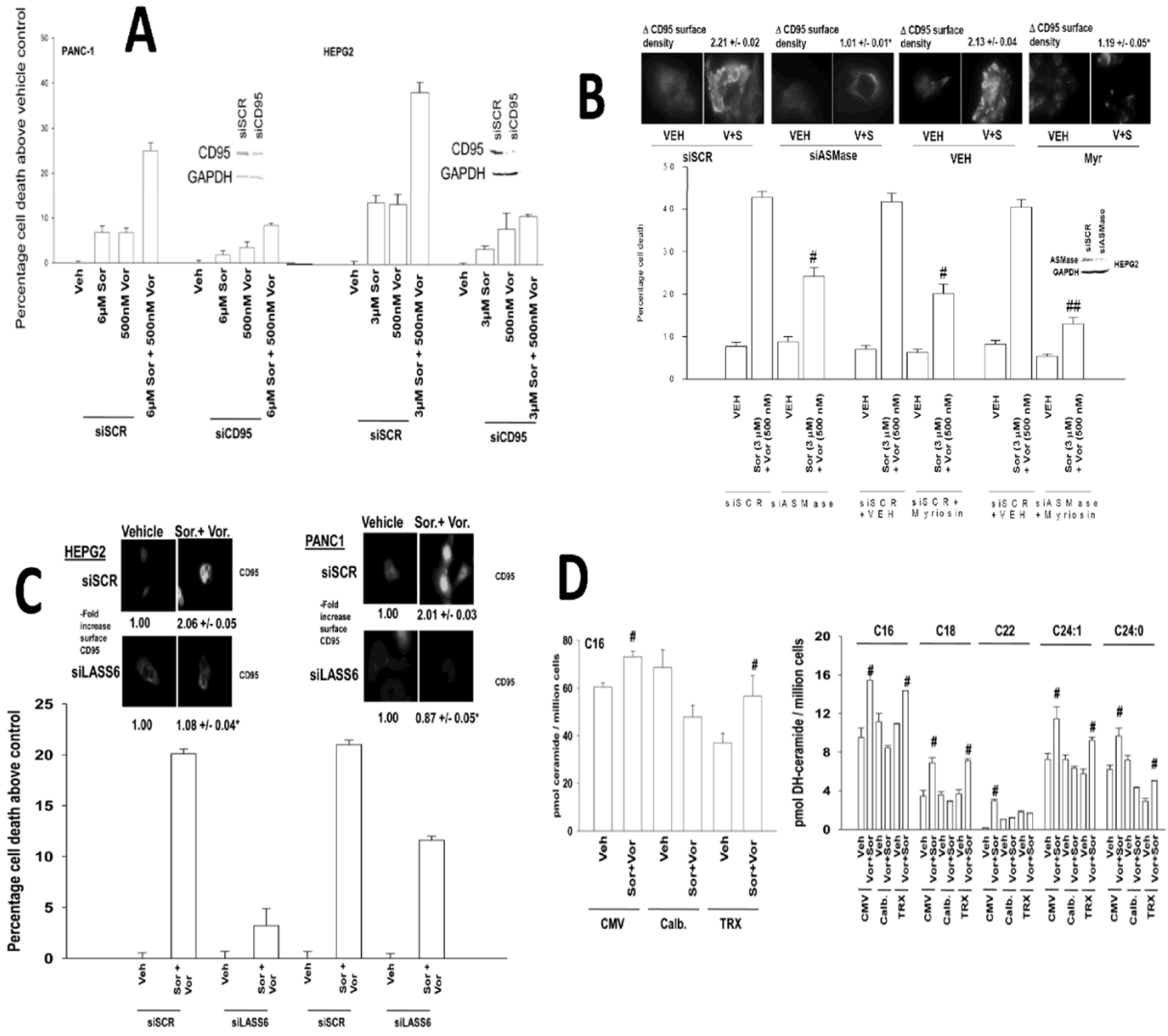

Figure 5. Co-dependent ceramide and Ca^{2+} regulation of CD95 activity and GI tumor cell killing

Panel A. HEPG2 and PANC-1 cells were transfected to knock down expression of CD95. Cells were treated 24h after transfection with sorafenib, vorinostat or both drugs. Viability was determined by trypan blue after 48h (n = 3, +/− SEM). **Panel B.** HEPG2 cells were transfected to knock down the expression ASMase. Cells were treated 24h after transfection with myriocin and 30 min later with sorafenib and vorinostat. *Upper IHC*, Cells were transfected as indicated and 24h later treated with drugs. Cells, after 6h cells were fixed and CD95 plasma membrane levels determined (n = 3, +/− SEM). *Lower graph:* 48h after exposure, viability was determined by trypan blue (n = 3, +/− SEM). **Panel C.** HEPG2 and PANC-1 cells were transfected to knock down expression of LASS6. Cells were treated 24h after transfection with sorafenib and vorinostat. *Upper IHC*, 6h after exposure cells were fixed and the levels of plasma membrane CD95 determined (n = 3, +/− SEM). *Lower graph:* 48h after drug exposure, viability was determined by trypan blue (n = 3, +/− SEM). **Panel D.** HEPG2 cells were transfected with plasmids to express Calbindin D28 or TRX. Twenty-four h after transfection cells were treated with sorafenib and vorinostat. Six h after treatment cells were taken and lysed and processed to isolate the lipid fraction of the cell. The levels of C16 ceramide and C16-C24:0 dihydroceramide were determined using a

tandem mass spectrometer as described in the Methods section (n = 2, +/− SEM) #p < 0.05 greater than corresponding vehicle treated value.

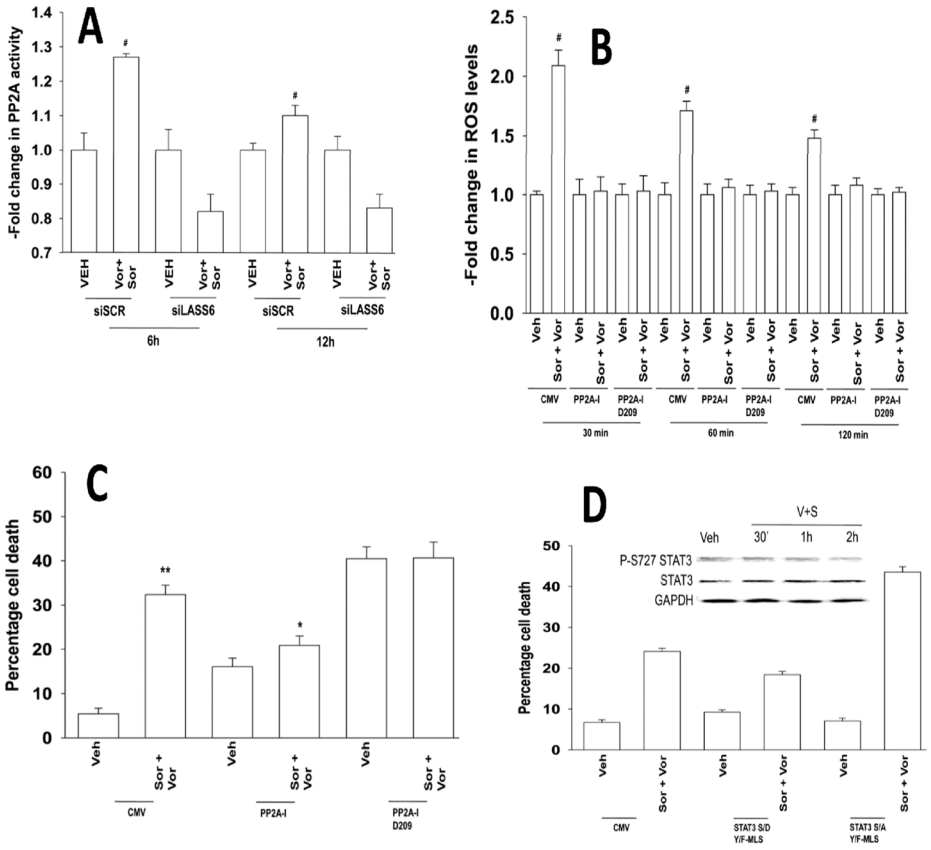

Figure 6. Sorafenib and vorinostat treatment activates PP2A in a LASS6-dependent fashion: PP2A activation is essential for enhanced ROS levels

Panel A. HEPG2 cells were transfected to knock down LASS6 expression (siLASS6). Twenty four h after transfection cells were treated with sorafenib and vorinostat. Cells were processed for PP2A activity according to the manufacturer's instructions. Data are the Fold change in PP2A activity (n = 2, +/− SEM) # $p < 0.05$ greater than corresponding vehicle treated value. **Panel B.** HEPG2 cells were transfected with plasmids to express wild type or mutant D209 PP2A-Inhibitor proteins. ROS levels were measured 15 min after drug exposure (n = 2, +/− SEM). **Panel C.** HEPG2 cells were transfected with plasmids to express wild type or mutant D209 PP2A-Inhibitor proteins. Twenty four h after transfection cells were treated with sorafenib and vorinostat. Cells were isolated and viability determined by trypan blue after 48h (n = 3, +/− SEM). **Panel D.** HEPG2 cells were transfected with plasmids to express mitochondria localized STAT3 S727A or STAT3 S727D. Twenty four h after transfection cells were treated with sorafenib and vorinostat. Viability was determined by trypan blue after 48h (n = 3, +/− SEM). Upper Inset: HEPG2 cells were treated with sorafenib and vorinostat and cells isolated at the indicated times and the levels of STAT3 S727, total STAT3 and GAPDH (n = 3).